

## Computational reconstruction techniques in integral imaging by use of a lenslet array

*Dong-Hak Shin, Eun-Soo Kim*

3D Research Center, School of Electronic Engineering, Kwangwoon University,  
447-1 Wolge-Dong, Nowon-Gu, Seoul 139-701, Korea, [shindh2@kw.ac.kr](mailto:shindh2@kw.ac.kr)

*ByoungHo Lee*

School of Electrical Engineering, Seoul National University  
Shinlim-Dong, Kwanak-Gu, Seoul 151-744, Korea

### Abstract

*In this paper, we propose novel computational reconstruction technique of three-dimensional objects in integral imaging by use of a lenslet array. We applied our technique to two different integral imaging systems according the distance between lenslet array and elemental image plane. Experimental results are presented and discussed as well.*

### 1. Introduction

Integral imaging (II) is one of the useful three-dimensional (3-D) image display techniques because it can produce true 3-D images with full parallax and continuous viewing points [1-5]. In II, the elemental images of a 3-D object are obtained by using a pinhole array (or a lenslet array) and a two-dimensional (2-D) image sensor such as the CCD (charge coupled device) camera. To reconstruct the 3-D image of an object, the elemental images are displayed on a display panel such as the LCD (liquid crystal display). The rays coming from the elemental images converge to form a real 3-D image through a pinhole array (or a lenslet array).

There are two types of analyses in II. One is the analysis using a pinhole array as shown in Fig. 1(a). This analysis is considered a single ray emitted from each pixel of display panel. This is useful in the applications of computer pickup and display [6,7]. The other is the analysis using a lenslet array as shown in Fig. 1(b). This is the case where the display panel has sufficient resolution. Each pixel of the display panel, then, is represented by properly light-emitting point. This analysis is useful to present the relation between depth and resolution [8-11] and also exploited in compensating the distortion of 3-D images according to depth [12].

Recently, various computational reconstruction II

techniques have been reported in order to obtain full 3-D volume information for image processing applications such as 3D surface extraction. These techniques are based on the analysis of II using a pinhole array. However, this conventional method can be applied only in small range of distances around the lenslet image plane (LIP) because off-focusing effect according to the distance is not considered in the conventional technique. When the reconstructed image plane is too far from the LIP, the off-focusing effect cannot be neglected, and consequently, the conventional method yields non-realistic result. The intensity irregularity with grid structures in the reconstruction image plane very close to lenslet array is one example of such non-realistic result.

In this paper, to overcome the problem of conventional technique, a new computational reconstruction technique in II using a lenslet array is proposed and some experimental results are also presented for showing the usefulness of the proposed technique.

### 2. Reconstruction technique in computational II using a lenslet array

We apply new computational reconstruction technique in II using a lenslet array to two II systems; depth-priority II (DP-II) and resolution-priority II (RP-II) [8].

Figure 2 illustrates the DP-II system. We obtain DP-II by use of real and virtual image fields when the distance  $g$  between lenslet array and display panel is  $f$ . The rays from pixels of a display panel become parallel through the lenslet array. The spot size  $D(z)$  of the integral point image in space is similar to lenslet size  $P$  regardless of the distance  $L$ . In other words,

$$D(z) = P. \quad (1)$$

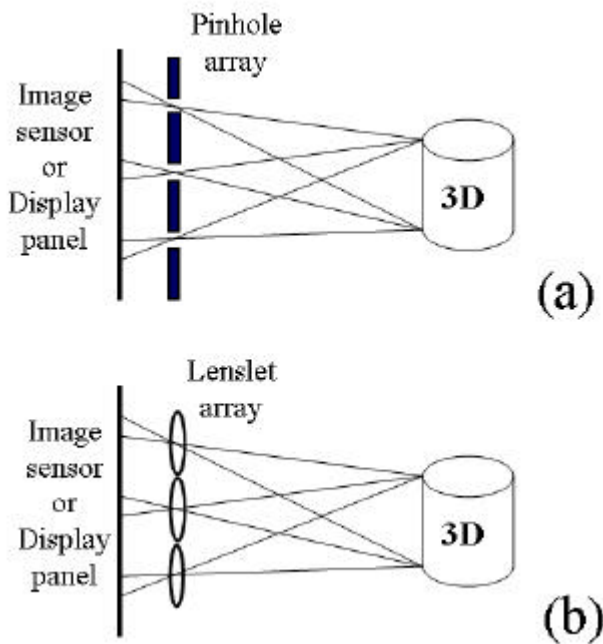


Fig. 1. II using (a) a pinhole array and (b) a lenslet array.

Figure 3(a) illustrates the RPII system based on the analysis of II using a lenslet array. The pixels  $d$  of display panel then are represented by properly light-emitting points on the display panel. For simplicity, a single lenslet model as shown in Fig. 3(b) is considered. From the Gauss lens law, the LIP is located at  $L=gf/(g-f)$ . With depth of focus  $\Delta z$  and diverging ray angle  $q$ , we can calculate the spot size  $D(z)$  of integral point image as following.

$$D(z) = \begin{cases} 2(L-z)\tan q, & \text{if } z \leq L - \Delta z; \\ 2L/d, & \text{if } L - \Delta z < z \leq L + \Delta z; \\ 2(z-L)\tan q, & \text{if } L + \Delta z < z. \end{cases} \quad (2)$$

In the proposed method, computational II reconstruction is obtained with a mapping procedure that all the pixels of the elemental images are projected and superposed with different spot size  $D(z)$  at the distance  $z$  to the reconstructed image plane through the lenslet array. Figure 4 illustrates our computational reconstruction procedure in detail. For a fixed distance  $z$  from the lenslet array, each pixel of elemental images is projected through each corresponding lenslet and is magnified according to the  $D(z)$ . The adjacent magnified pixels are overlapped each other at the reconstructed image plane. For all the pixel of the elemental image, the same procedure is repeated and computed with

overlapping each other. Then we can obtain one reconstructed image at the distance  $z$ . To generate 3-D volume information, the mapping procedure is repeated for all reconstructed planes of interest.

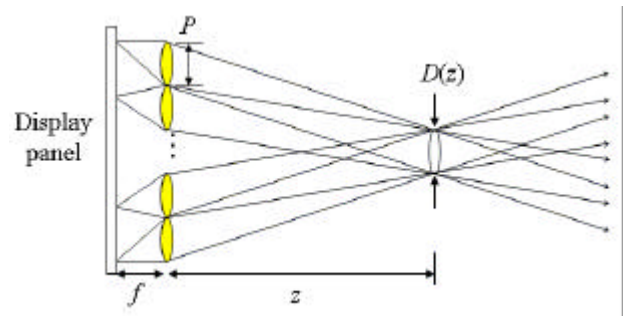


Fig. 2 DPII system by use of both real and virtual image fields.

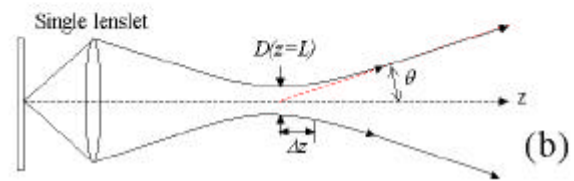
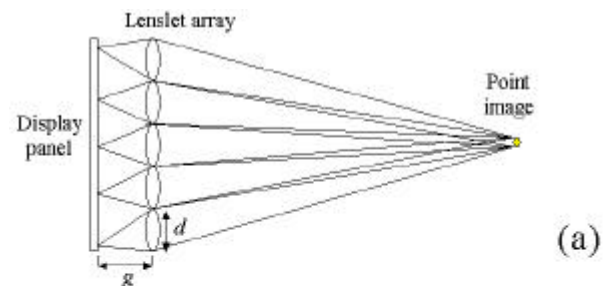


Fig. 3 (a) RPII system using a lenslet array. (b) Ray formation by single lenslet

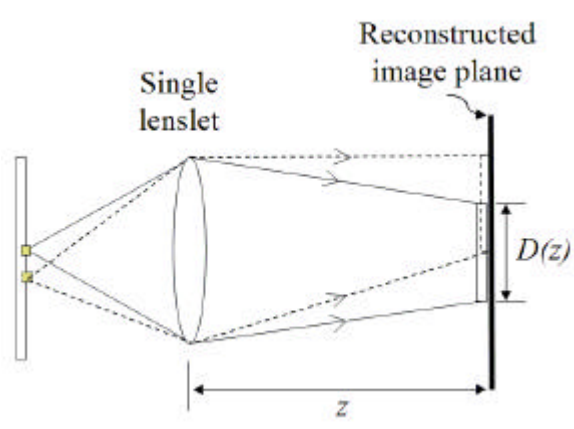


Fig. 4 Mapping procedure of elemental images

### 3. Experimental results

To test the performance of the proposed reconstruction technique, computational experiments are carried out for both DPII system and RPII system.

#### 3.1 DPII

To demonstrate the proposed reconstruction technique in DPII, we used the experimental structure as shown in Fig. 5. Here the focal length  $f$  of the lenslets is 3 mm and is the same that the gap  $g$  between the display panel and the lenslet array. Then we obtain DPII system.

We used a 3-D object composed of four 2-D character patterns, 'I', 'T', 'R' and 'C' whose size is 1020×750 pixels. The patterns are longitudinally located at +90 mm, +30 mm, -3 mm and -45 mm from the origin of lenslet array, respectively. The lenslet array has 34×25 lenslets whose size is 1 mm. Each lenslet is 30×30 pixels.

After synthesizing elemental images for the use in the experiment, the reconstruction was performed. Each pixel from elemental images was uniformly mapping with the size of 3 mm into the reconstructed image plane. Entire reconstruction image was obtained by repeating all the pixels of elemental images. Figure 6 are the computationally reconstructed images at various display planes using the proposed reconstruction technique. Eight reconstructed images at the distance of +90, +45, +30, 0, -3, -30, -45 and -90 mm are shown in Fig. 6(a)-6(h), respectively. We can see clear images at +90, +45, -3 and -45 mm which are the image display planes of the patterns. However we can see blurred images at other distances.

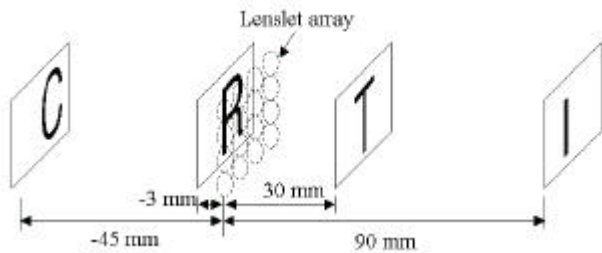


Fig. 5 Experimental conditions for DPII system.

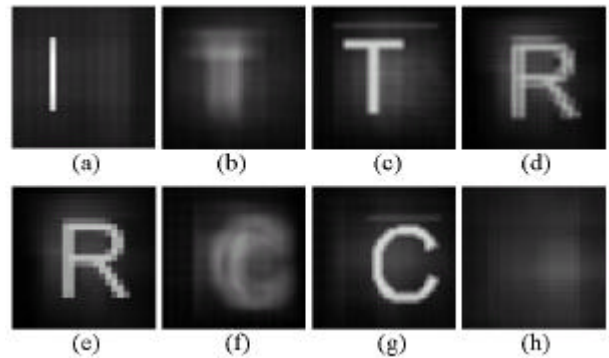


Fig. 6 Reconstructed images in DPII system.

#### 3.2 RPII

For RPII system as shown in Fig. 3, an experimental structure of the computational reconstruction is shown in Fig. 7. In the experiment, a test object composed of two alphabetical patterns, 'P' and 'K' is used. The 'P' and 'K' alphabetical patterns are longitudinally located at  $z=23$  cm and  $z=33$  cm, respectively. The focal length  $f$  of the lenslet is 3 cm and the gap  $g$  between the display panel and the lenslet array is 3.3 cm. In this case,  $g \neq f$ . Therefore this is RPII system.

By using the synthesized elemental images, the 3-D images were reconstructed computationally. Figure 8 shows the computationally reconstructed images at various display planes. Reconstructed images at the distance of  $z=3.3, 23, 33$  and 66 cm are shown in Fig. 8(a)-8(d), respectively. We can see clear images at  $z=23$  and 33 cm which are the image display planes of the patterns. From the results, we believe that our experiment was successfully demonstrated

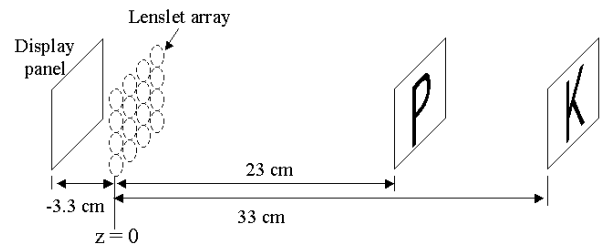


Fig. 7 Experimental conditions for RPII system.

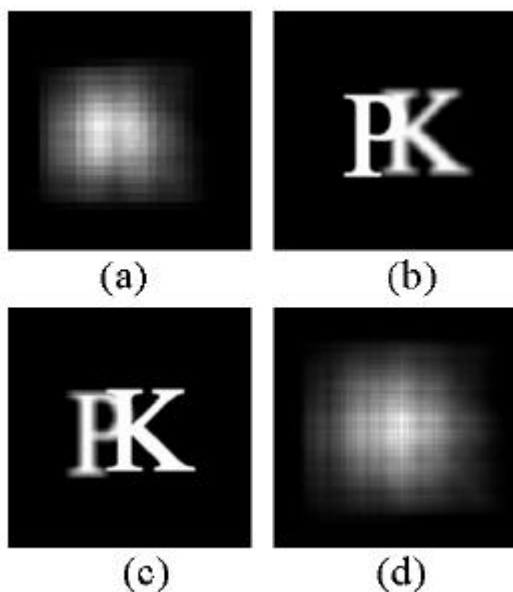


Fig. 8 Reconstructed images in RPII system.

#### 4. Conclusion

In this paper, we propose novel computational reconstruction technique of three-dimensional objects in integral imaging by use of a lenslet array. Our technique can be applied to two different integral imaging systems; DPII and RPII. We introduced conventional computation reconstruction technique to variable mapping size and presented the usefulness of proposed technique through experimental results.

#### 5. Acknowledgements

This research works was supported by ITRC project of Korea Ministry of Information and Communication.

#### 6. References

- [1] G. Lippmann, "La photographie integrale," *Comptes-Rendus Academie des Sciences* 146, 446-451 (1908).
- [2] F. Okano, H. Hoshino, J. Arai, and I. Yuyama, "Real-time pickup method for a three-dimensional image based on integral photography," *Appl. Opt.* 36, 1598-1603 (1997).
- [3] J.-S. Jang and B. Javidi, "Improved viewing resolution of three-dimensional integral imaging with nonstationary micro-optics," *Opt. Lett.* 27, 324-326 (2002).
- [4] B. Lee, S. Jung, S.-W. Min, and J.-H. Park, "Three-dimensional display by use of integral photography with dynamically variable image planes," *Optics Letters*, vol. 26, no. 19, pp. 1481-1482, 2001.
- [5] D.-H. Shin, M. Cho and E.-S. Kim, "Computational implementation of asymmetric integral imaging by use of two crossed lenticular sheets," to be accepted in *ETRI journal*.
- [6] H. Arimoto and B. Javidi, "Integral three-dimensional imaging with digital reconstruction," *Opt. Lett.* 26, 157-159 (2001).
- [7] S.-H. Hong, J.-S. Jang and B. Javidi, "Three-dimensional volumetric object reconstruction using computational integral imaging," *Opt. Exp.* 12, 483-491 (2004).
- [8] J.-S. Jang, F. Jin and B. Javidi, "Three-dimensional integral imaging with large depth of focus by use of real and virtual image fields," *Opt. Lett.* 28 1421-1423 (2003).
- [9] F. Jin, J.-S. Jang and B. Javidi, "Effects of device resolution on three-dimensional integral imaging," *Opt. Lett.* 29 1345-1347 (2004).
- [10] J.-H. Park, S.-W. Min, S. Jung, and B. Lee, "Analysis of viewing parameters for two display methods based on integral photography," *Appl. Opt.* 40, 5217-5232 (2001).
- [11] B. Lee, S.-W. Min, and B. Javidi, "Theoretical analysis for three-dimensional integral imaging systems with double devices," *Appl. Opt.* 41, 4856-4865 (2002).
- [12] J. Hong, J.-H. Park, J. Kim, and B. Lee, "Analysis of image depth in integral imaging and its enhancement by correction to elemental images," *Novel Optical Systems Design and Optimization VII*, SPIE Annual Meeting, Proc. SPIE, vol. 5524, Denver, Colorado, USA, pp. 387-395, Aug. 2004.